Redox Controls over the Stability of U(IV) in Floodplains of the Upper Colorado River Basin

Vincent Noël[†], Kristin Boye[†‡], Juan S. Lezama Pacheco[†‡], Sharon E. Bone[†], Noémie Janot[†], Emily Cardarelli[‡], Kenneth H. Williams[§], and John R. Bargar[*†]

[†] Stanford Synchrotron Radiation Lightsource, SLAC National Accelerator Laboratory, Menlo Park, California 94025, United States

[‡] Department of Environmental Earth System Science, Stanford University, Stanford, California 94305, United States

[§] Earth Sciences Division, Lawrence Berkeley National Laboratory, Berkeley, California 94720, United States

*E-mail: bargar@slac.stanford.edu.

Abstract

Aquifers in the Upper Colorado River Basin (UCRB) exhibit persistent uranium (U) groundwater contamination plumes originating from former ore processing operations. Previous observations at Rifle, Colorado, have shown that fine grained, sulfidic, organic-enriched sediments accumulate U in its reduced form, U(IV), which is less mobile than oxidized U(VI). These reduced sediment bodies can subsequently act as secondary sources, releasing U back to the aquifer. There is a need to understand if U(IV) accumulation in reduced sediments is a common process at contaminated sites basin-wide, to constrain accumulated U(IV) speciation, and to define the biogeochemical factors controlling its reactivity. We have investigated U(IV) accumulation in organic-enriched reduced sediments at three UCRB floodplains. Noncrystalline U(IV) is the dominant form of accumulated U, but crystalline U(IV) comprises up to ca. 30% of total U at some locations. Differing susceptibilities of these species to oxidative remobilization can explain this variability. Particle size, organic carbon content, and pore saturation, control the exposure of U(IV) to oxidants, moderating its oxidative release. Further, our data suggest that U(IV) can be mobilized under deeply reducing conditions, which may contribute to maintenance and seasonal variability of U in groundwater plumes in the UCRB.

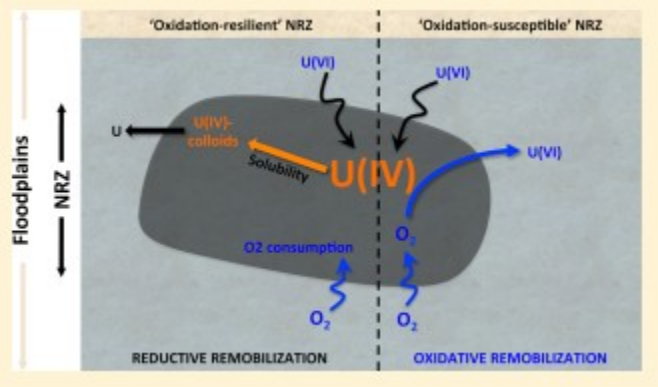

Introduction

Uranium (U) is a persistent contaminant in groundwater at legacy ore-processing sites in the Upper Colorado River Basin (UCRB).(1-3) Plumes at these sites exhibit U concentrations exceeding the maximum concentration limit (MCL; 0.044 mg_U/L), and are not self-attenuating through the natural flushing of groundwater as originally expected.(3) For example, estimates suggest U concentrations in groundwater at the Rifle site, CO, could remain above this regulatory limit for tens if not hundreds of years.(3, 4) The specific mechanisms responsible for plume persistence are not known. However, field observations such as at the Riverton, WY site(5, 6)suggest that sediments in hydrological contact with the aquifer have accumulated U and are releasing it back to the groundwater. Research is required to elucidate the underlying mechanisms, at local and regional scales, in order to appropriately manage and remediate these sites.

Studies at the former U ore processing site at Rifle, CO, have shown that sulfidic organic-enriched sediment lenses strongly accumulate U(IV), obtaining concentrations >200-fold higher than background.(4, 7, 8) Sulfidic sediments, referred to as “naturally reduced zones” or NRZs,(9)locally create conditions that can promote abiotic reduction of U(VI) to U(IV)(10-20) and biologically mediated reduction.(21-28) Recent laboratory model studies(29) suggest that both abiotic and biotic reduction pathways operate in NRZs, but that U(IV) reduction is predominantly accomplished through direct biological activity. U(IV) is relatively insoluble, and thus accumulates in sediments, emphasizing the importance of reducing conditions to U retention.(4, 7, 30) Recent studies show that NRZs occur at U-contaminated sites at Grand Junction and Naturita, CO, Moab, UT, and Riverton, WY,(6, 9, 31, 32) raising the question of whether or not NRZs are regionally important for accumulating U in the UCRB.(4) Here, we examine uranium data from NRZs at other field sites in the upper CRB to address this question.

In a previous study,(9) we identified two main classes of NRZs in the UCRB, both exhibiting elevated organic matter content compared to surrounding sediments, but differing in terms of particle size and water saturation. Reduced sediments from Rifle typify “fine-grained” NRZs, which are enriched in the <150 µm sediment size fraction compared to surrounding sediments, creating strong permeability contrasts and sharp redox gradients. Rifle NRZs are saturated year-round, and exhibit stable reducing conditions as characterized by the presence of abundant mackinawite (FeS), in addition to pyrite (FeS_2). In contrast, “coarse-grained” NRZ exhibit grain size distributions are similar to those in under- and overlying sediments, leading to more dynamic exchange of oxidants with surrounding aquifers and seasonal redox cycling(9) (Figure 2). As a result, “coarse-grained NRZs” contain elemental sulfur and pyrite, but lack mackinawite.(9)

The contrast in NRZ characteristics implies that associated uranium speciation, abundance, and mobility may also exhibit contrasting behaviors.

Thus, the development of regionally applicable models for uranium mobility in organic-enriched sediments requires understanding the behavior of U in these different NRZ classes. Incursion of oxidants, such as O_2 and NO_3^-, into coarse-grained NRZs has the potential to reverse their roles from U sinks to secondary sources U through U(IV) oxidation and subsequent release of U(VI).(3) The chemical and physical form (e.g., adsorbed or crystalline) of U(IV) strongly mediates its chemical stability(33, 34) and, thus, its release from sediments. U(IV) sorbed on biomass(29) or mineral surfaces(35) is expected to be more susceptible to oxidation than biogenic uraninite (UO_2; (33, 34)). Moreover, U release can also occur under reducing conditions.(36-39) The varying reactivity of different U(IV) species to remobilization creates a need to assess speciation in contaminated sediments. Knowledge of the biogeochemical and physical controls promoting the formation and mobilization of each type of U(IV) product would be particularly valuable, as it would improve our ability to predict the behavior of accumulated U(IV) in data-poor sites without direct analyses of U speciation.

The objectives of the present study were to (a) Evaluate and compare U accumulation capacities of NRZ sediments within and across multiple sites across the UCRB; (b) Distinguish between noncrystalline and crystalline forms of U(IV) and determine their distribution in these sediments; and (c) Constrain the biogeochemical factors governing the accumulation and mobilization of U. Sediments were collected from three field sites: Rifle, Naturita, and Grand Junction, CO,(9)covering a linear distance of 250 km through the central portion of the UCRB. Knowledge produced by this work supports the development of conceptual and numerical models of U behavior and transport within floodplains and provides critical insights to management and remediation efforts at sites where characterization data may not exist.

Materials and Methods

Field Sites Description

The Rifle, Naturita, and Grand Junction, CO, sites are DOE-managed former U ore processing facilities(3, 40-48) located in the central portion of the UCRB (Figure SI-1 in Supporting Information). The Rifle site is approximately 0.50 km east of the city of Rifle along the Colorado River. The Naturita site is located approximately 3.22 km north of the town of Naturita, CO along the San Miguel River. The Grand Junction former mill site is located along the north bank of the Gunnison River near the confluence with the Colorado River. Surface remediation was initiated in the mid-1980s at the Grand Junction site under the Formerly Utilized Sites Remedial Action Program (FUSRAP) and in mid-1990s at Rifle and Naturita, under the Uranium Mill Tailings Radiation Act (UMTRA).

Sampling of Sediment Solids and Porewater

Sediment cores were obtained through rotosonic drilling (Rifle, August 2014) or direct push coring (Grand Junction, Naturita, October 2014) and retrieved

in N_2-purged plastic sleeves. In total, four cores containing NRZ materials were selected for this study; two cores (748 and 753) from Rifle, one core (NAT-M8–1) from Naturita, and 1 core (GJAST15B) from Grand Junction (see Figures SI-2, SI-3, and SI-4). These new cores, obtained from the far western portion of the Rifle site, allow further evaluation of U accumulation and speciation across the site, because they can be compared to formerly published results from cores collected from the center portion of the site (170 m distant).

Porewater was immediately extracted from sediment cores using Rhizon soil moisture samplers.(49) All porewater samples were anaerobically preserved under Ar, shipped on ice, and stored in the dark at 3 °C until analysis. Following porewater collection, the sediment samples were collected every 10 to 40 cm from surface to bedrock (ca. 930 cm bgs for Rifle, and 500–600 cm bgs for Grand Junction and Naturita). Sediment samples that visibly appeared to be darkened by the presence of sulfides and smelled sulfidic were collected at finer vertical resolution (~5 cm), along with a segment of neighboring over- and underlying sediment, under Ar flow and preserved from oxidation in Ar-purged serum vials (crimp-sealed with rubber stoppers). All samples were immediately stored in the dark, shipped on ice, and vacuum-dried in a glovebox 5%H_2/95%N_2atmosphere as reported previously. (9) After drying, each sediment sample was sieved (<1 mm), homogenized, and stored in sealed containers in an anoxic glovebox.

Sampling of Groundwater

Groundwater was passively sampled using equilibration dialysis devices, commonly called “peepers”, following a protocol derived from Johnston et al. (50) The concept is illustrated (Figure SI-5) and explained in detail in the SI. Cells were deoxygenated, filled with anoxic Milli-Q water and maintained in immersion until field deployment.(50) Peeper design was optimized so that the time required to reach cell equilibration with groundwater was less than 15 days, and the material used to manufacture the peepers was chosen to avoid contamination from molecular oxygen, metals, and DOC. The peeper structure was installed directly in existing wells nearby the sediment sampling locations (NAT-M8 and NAT-M4; Figure SI-3), with peeper membranes (0.2 μm polypropylene) exposed to the natural groundwater flow (Figure SI-5). The peepers were replaced after each sampling, and groundwater from the depths of peeper installations was pumped to the surface using a peristaltic pump to measure the oxidation reduction potential (ORP) using a YSI 556 MPS multiprobe system, systematically before the time of retrieval.

Chemical and Mineralogical Analyses

Bulk sediments were analyzed for their chemical compositions using X-ray fluorescence spectrometry with a XEPOS (Spectro X Lab) X-ray fluorescence spectrometer. Their organic carbon (OC) content was determined with Carlo Erba NA1500 elemental analyzer. The chemical and organic compositions of

the bulk sediments were previously described in detail in Noël et al.(9) Because the chemical forms of S and Fe exhibit dramatic variability tied to redox conditions, they comprise efficient and precise tracers of mineral transformations in the floodplain sediments of UCRB.(4, 7-9) The speciation of S and Fe in the sediment cores included in this study was previously examined and reported in Noël et al.,(9) and used here as indicators of sediment redox status. S mineralogical composition was determined using X-ray absorption spectroscopy combined with X-ray microprobes, and the Fe mineralogical composition was analyzed using X-ray absorption spectroscopy combined with mössbauer spectroscopy. To supplement the data from Noël et al.,(9) synchrotron powder X-ray diffraction (SR-XRD) was performed on the sediments as part of this study. Porewater and groundwater samples were analyzed for their element composition using high-resolution inductively coupled plasma mass spectroscopy (HR-ICP-MS). The analytical procedures are reported in the SI.

U Speciation

Chemical Extractions

Sequential chemical extractions of sediments were performed in (i) anoxic Milli-Q water (water-extractable fraction), (ii) anoxic bicarbonate solution (organic-complexed and/or mineral-adsorbed fraction), (iii) aqua regia ("recalcitrant" or crystalline fraction); to assess the U distribution between "recalcitrant" or crystalline U and more labile forms of U according to a protocol derived from Alessi et al.(51) Based on the greater lability of organic-complexed and adsorbed U compared to crystalline U,(33) the anoxic bicarbonate extraction method effectively distinguishes between these species in environmental samples such as NRZs.(51)

X-ray Absorption Spectroscopy (XAS)

U L_{II}-edge X-ray absorption near-edge structure (XANES) spectroscopy was used to determine U oxidation states. Extended X-ray absorption fine structure (EXAFS) spectra were examined to constrain the local molecular structure around U whenever its concentrations were sufficiently high (≥20 μg/g). The U L_{II}-edge was preferred to U L_{III}-edge to avoid interference of the uranium Lα fluorescence peak (=13614 eV) with the rubidium fluorescence Kα peak (=13396 eV). Fluorescence-yield XANES and EXAFS spectra were collected using a 100 pixel germanium X-ray detector at beamline 11–2 at Stanford Synchrotron Radiation Ligthsource (SSRL). The samples were loaded in an Al sample holder with Kapton windows inside an anaerobic chamber (3% hydrogen, balance nitrogen). Immediately prior to analysis, the sample was transferred from the anaerobic chamber and mounted in a liquid N_2 cryostat, placed under vacuum, and cooled to 77 K. A Si (220) double-crystal monochromator was detuned to reject higher harmonic intensity. Energy was calibrated with Mo foil recorded in double transmission setup, by setting the first inflection point in the K-edge to 20000 eV. 6–25 scans were recorded for each sample. U L_{II}-edge data were averaged, normalized, and

analyzed by linear combination-least-squares (LC-LS) fitting using the ATHENA software.(10, 52) To enable comparison of spectra measured at different beamlines, the vertical limiting aperture was set small enough that the spectrometer resolution was much lower than the energy corresponding to the core-hole lifetime (ca. 9 eV). Our U model compounds data set includes U(VI) as andersonite ($Na_2Ca(UO_2)(CO_3)_3 \cdot 6H_2O$; 4), crystalline U(IV), (53) as well as U(IV) complexes bound to OM-clay aggregates(29) and U(IV) complexes bound to biomass through P- and/or C-containing ligands.(26) The quality of the LC-LS fits was estimated using an R-factor of the following form: $Rf = \Sigma [k^3\chi(k)_{exp} - k^3\chi(k)_{calc}]^2/\Sigma [k^3\chi(k)_{exp}]^2$. The accuracy of the XANES fitting procedure is estimated to be ±5% of the fit-determined.(54) The components below 5% are thus considered as not significant.

Results

Mineral and Organic Composition of the Floodplain Sediments

Bulk sediment characteristics of the cores from Rifle, Naturita, and Grand Junction were previously described in detail(9) and are schematically summarized in Figure 1e,f and Figure SI-6. The mineralogy was dominated by quartz (SiO_2), and feldspar minerals, such as albite ($NaAlSi_3O_8$; Figure SI-6, SI-7). A small amount of chloritoids, such as ottrelite ($(Mn,Fe,Mg)_2Al_4Si_2O_{10}(OH)_4$)) was also identified (Figure SI-6, SI-7). Mössbauer and XAS show the presence of hematite (α-Fe_2O_3), magnetite (Fe_3O_4), goethite (α-FeO(OH)), Fe(II)- and Fe(III)-bearing clays, and sulfate minerals (ref 9, Figure SI-6). At each of these field sites, OC- and sulfide-enriched sediment lenses were identified as NRZs (Figure SI-6, ref 9). Strong redox gradients were evident at the interface between NRZs and surrounding aquifers. Along these gradients, goethite and sulfate minerals decreased in abundance toward the interior of the NRZs and were replaced by iron sulfides. The redox characteristics, organic content and mineral compositions of NRZs at Rifle, Naturita, and Grand Junction were previously detailed in Noël et al.(9) and are schematically summarized in Figure 1e,f,g. The two main classes of NRZ previously defined by Noël et al.(9) are also schematically illustrated in Figure 2. Rifle NRZs are the “type” example of fine-grained NRZs. In contrast, Naturita and Grand Junction NRZs constitute the “type” examples of coarse-grained NRZs.

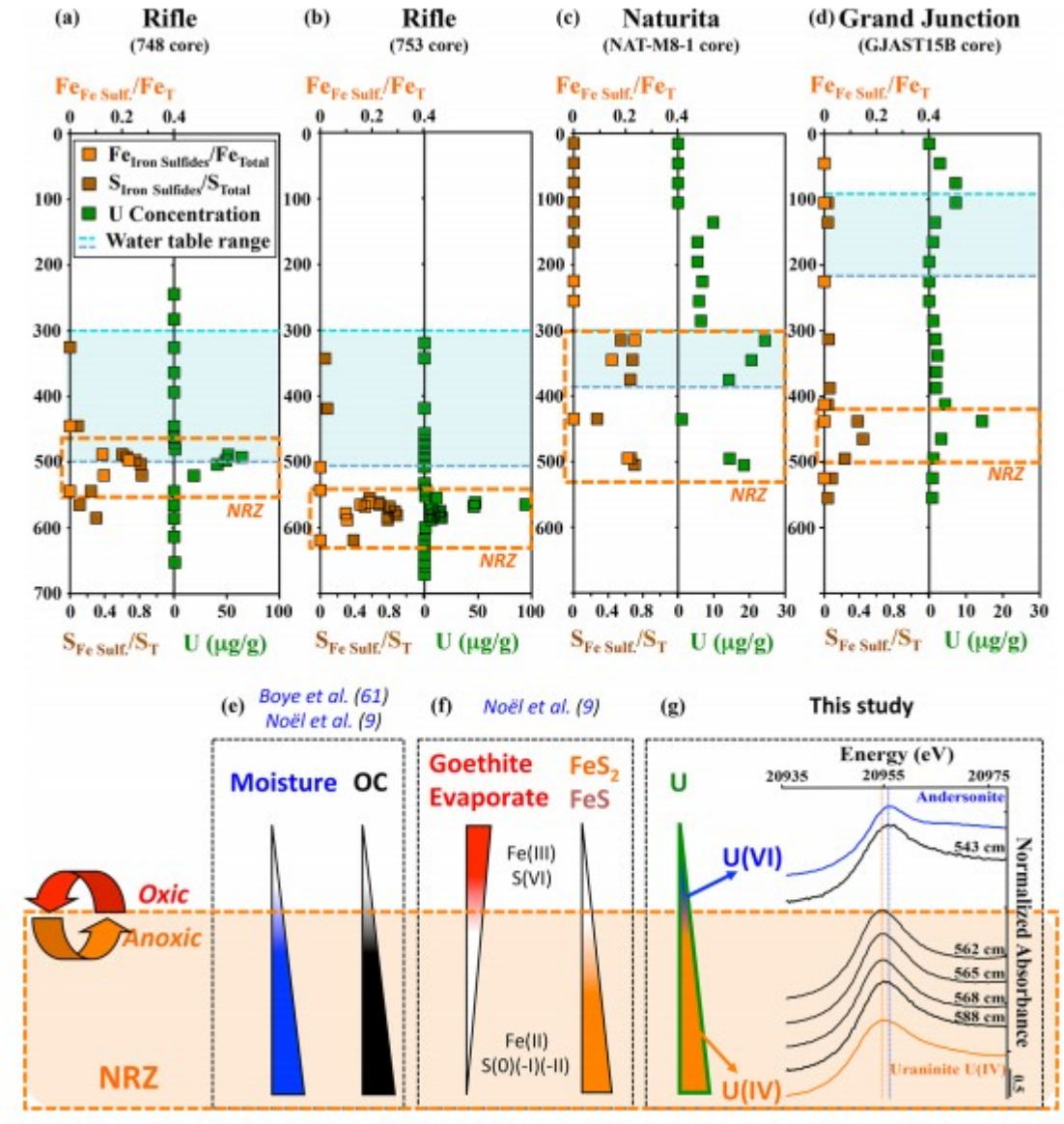

Figure 1. Comparison of U and iron sulfide bulk concentration profiles indicating locations of NRZs at: Rifle (a and b), Naturita (c), and Grand Junction (d). For each panel (a,b,c,d), the composition profiles (left) show the distribution of Fe as iron sulfides normalized to total Fe (red) and the distribution of S as iron sulfides normalized to total S (brown). Composition profiles on the right show bulk sediment total U (green). Fe, S, and U concentrations are reported in Table SI-1. Blue dotted lines indicate the minimum (Min.) and maximum (Max.) levels of the groundwater table; Orange lines and shading denote the elevations of the NRZs. Lower panel illustrates average characteristics of NRZ sediments at Rifle, Naturita, and Grand Junction: redox conditions (vertical wedges depict variability in the abundances), (e) moisture and organic carbon are required to establish NRZs;(9, 61) (f) goethite is generally replaced by iron sulfides;(9) and (g) (data from the Rifle 753 core) total uranium and U(IV) increase inside NRZs. The relative proportions of U(VI) and U(IV) in individual samples are provided for each core in Figure SI-8.

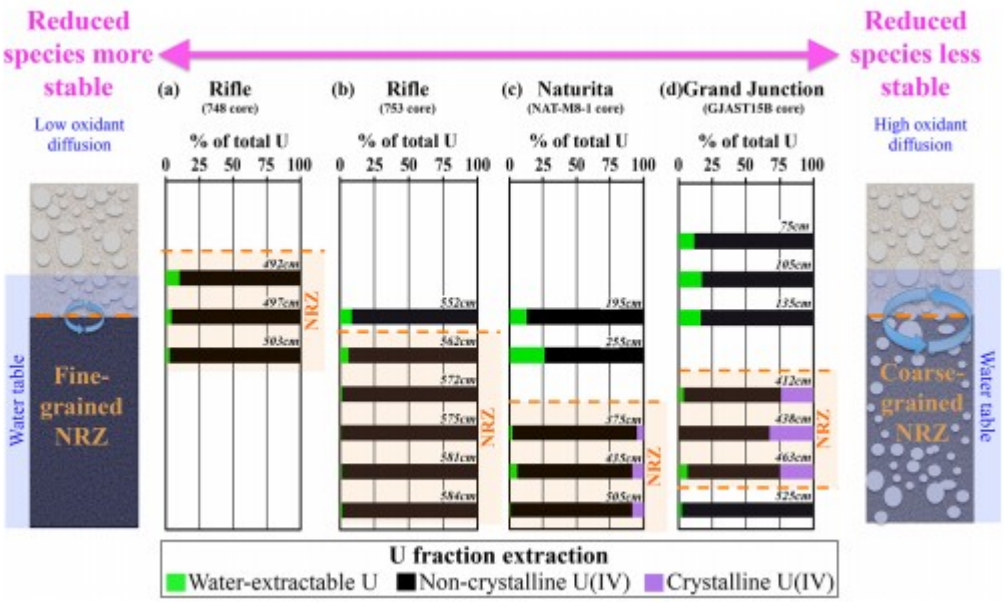

Figure 2. Distribution profiles of U species in the bulk sediment samples from the three U-contaminated floodplains as a function of depth. Bar plots show the extracted U fractions, for Rifle (a and b), Naturita (c), and Grand Junction (d), with the relative proportion of exchangeable U (green), noncrystalline U(IV) (black), and crystalline U(IV) (purple) normalized to 100%. The corresponding U content in each fraction is reported in SI Table SI-2. Orange lines and shading denote the location of the NRZs. The left- and right-hand schema summarizes the sediment texture, organic carbon content, and saturation state of fine-grained (Rifle) and coarse-grained (Naturita and Grand Junction) NRZs, respectively.(9)

Vertical Distribution of U and Redox Conditions

NRZs are distinguishable in sediment profiles by the presence of iron sulfides [FeS and FeS_2] (ref 9; Figure 1f). Thus, to examine the relevance of NRZs for U accumulation, the concentration of S and Fe as iron sulfides, normalized to that of total S and Fe, respectively, are plotted along with the vertical profiles of U for the collected cores from Rifle, Grand Junction, and Naturita in Figure 1a,b,c,d.

Horizons with elevated U content were present in all cores. U concentrations increased from an average of ~0.5 μg/g in the aquifer sediments up to 60 and 100 μg/g in the 748 and 753 cores of Rifle fine-grained NRZs (Figure 1a,1b), and up to 20 μg/g and 10 μg/g in coarse-grained NRZs of Naturita (Figure 1c) and Grand Junction (Figure 1d), respectively. Sediment U concentrations systematically covaried with organic carbon and with iron sulfides regardless of the NRZ type (Figure 1e,f,g). However, the total U concentrations measured in the Rifle fine-grained NRZs were 3- to 10-fold higher than total U concentrations in the Naturita and Grand Junction coarse-grained NRZs. It is worth noting that we also observed U concentrations slightly higher than background in the shallow unsaturated zone, coinciding with abundant evaporite minerals; sediments above the groundwater table from Naturita and Grand Junction exhibited U concentrations ≤5.7 μg/g (100–300 cm bgs in NAT-M8–1 and 30–100 cm in GJAST15B) (Figure 1c,1d). This

modest U-accumulation does not appear to result from redox transformations and will be covered in a separate paper.

According to the U L_{II}-edge XANES spectra, U in all NRZ samples was dominated by U(IV) independent of NRZ type; On average U(IV) comprised 95 ± 5% of total U, ranging from 89 ± 5% to 100 ± 5% (Figure SI-8). In contrast, oxidized (non-NRZ) sediments contained 45 ± 5% to 53 ± 5% U(IV) (Figure SI-8). An example of a fine-grained NRZ U profile is detailed in Figure 1g (Rifle core 753). Despite very low concentration (~1 µg/g), the occurrence of U(IV) in oxidized aquifer sediments suggests that the high heterogeneity of sediment textures and chemical/mineralogical compositions may maintain reducing conditions in the interior of aggregates comprising of organic-enriched sediments in physical juxtaposition with aquifer sediment. (55) At Rifle, Janot et al.(4) also reported the presence of a significant amount of mackinawite in the capillary fringe above the NRZ, supporting this hypothesis.

U Extractions: Noncrystalline U(IV) vs Crystalline U(IV)

U L_{II}-edge XANES results show that U is dominantly present as U(IV) in NRZs. Consequently, we interpret (i) water-extractable “NRZ” uranium as weakly sorbed U(IV) (anoxic Milli-Q water); (ii) HCO_3-extractable uranium is interpreted as noncrystalline U(IV), organic-complexed and/or strongly mineral-adsorbed (anoxic HCO_3 extraction); and (iii) “recalcitrant” uranium is interpreted as crystalline U(IV) (aqua regia). The results of the chemical extractions of U from NRZs are shown in Figure 2 (values are reported in Table SI-2). The water-extractable U fraction comprised only a small portion of total U, reaching an average of 12% in non-NRZ sediments (where U(VI) also was present) and decreasing from the interface with aquifer sediments to the interior of the NRZs (from an average of 6% to an average of 1%; Figure 2), consistent with a lower solubility of U(IV) as compared to U(VI). At all three sites, noncrystalline U(IV) was the dominant fraction (between 67% and 99%; Figure 2) in NRZs. The fine-grained NRZs from Rifle (cores 748 and 753) contained no detectable crystalline U(IV). In contrast, crystalline U(IV) comprised an average of 7% and 27% of total U in the coarse-grained NRZs of the NAT-M8–1 core from Naturita and the GJAST15B core from Grand Junction, respectively.

EXAFS Evidence for Noncrystalline U(IV)

Rifle NRZ samples were selected for EXAFS analysis to gain information about the local bonding environment of U that could help constrain and interpret the extraction results. EXAFS spectra and their corresponding Fourier Transforms (FTs) are displayed in Figure 3. Owing to low U concentrations (<100 µg/g), the EXAFS spectra were considered too noisy after 8 $Å^{-1}$. In spite of this short *k*-range, the EXAFS data can be used to exclude several U(IV) phases from consideration. Referring to the EXAFS spectra in Figure 3, we can see that there are important differences between the EXAFS for UO_2 and for our spectra. The UO_2 EXAFS contain multiple

strong frequencies (corresponding to multiple pair correlations), whereas ours spectra have one dominant frequency (i.e., U–O). In particular, the UO_2 EXAFS spectra exhibit a sharp valley at ca. 7.3 $Å^{-1}$ and a sharp peak at ca. 7.6 $Å^{-1}$,(26, 53, 56) neither of which are present in our field sample spectra. A similar pair of “peak–valley” features are present in coffinite ($U(SiO_4)_{1-x}(OH)_{4x}$) and U(IV)-silicate colloids.(57) EXAFS spectra are highly sensitive to local molecular structure around U. Consequently, these differences indicate that crystalline U(IV) and U(IV)-silicate colloids are absent from the Rifle samples above detection limit (ca 15% of total U species).

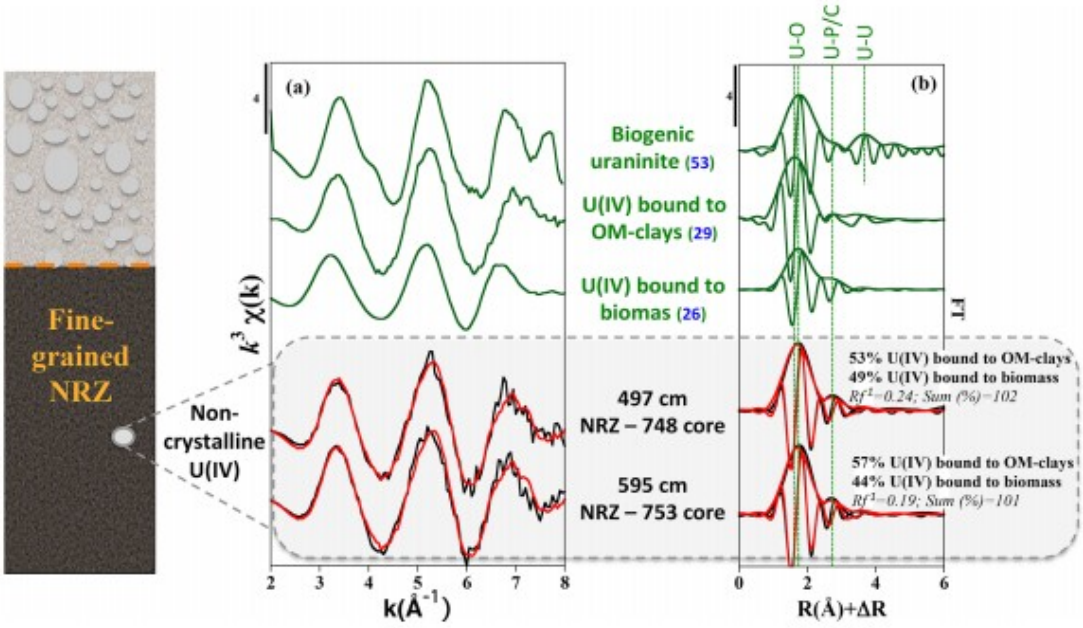

Figure 3. Lower panels display experimental k^3-weighted U EXAFS data (a) and corresponding Fourier transforms (b) of samples from Rifle NRZs (black lines) and LC-LS fits (red lines). EXAFS spectra for model compounds used for LC-LS fits are provided above the sediment data, and biogenic uraninite is shown for indicating that the distinctive frequencies between 7 and 8 $Å^{-1}$ are not present in the NRZ sample spectra. The left-hand schema summarizes the sediment texture, organic carbon content, and saturation state of Rifle fine-grained NRZs. [1]*Fit quality was estimated by a R-factor calculated as* $Rf = \Sigma [k^3\chi(k)_{exp} - k^3\chi(k)_{calc}]^2 / \Sigma [k^3\chi(k)_{exp}]^2$.

Thus, the EXAFS is consistent with the extraction conclusions that U(IV) occurred as noncrystalline U(IV). Bone et al.(29) showed that U(IV) was complexed primarily to organic matter functional groups in simulated NRZ sediments. Similar to those results, our FT-EXAFS spectra show a first coordination shell U–O pair correlation characterized at 2.32–2.34 Å using shell-by-shell fitting (see SI, Table SI-3). A minor frequency is present in our data at 2.65 Å (R+dR; Figure 3b), which can be fit with C neighbors at 2.85 Å(58) or with P neighbors at 3.08 Å.(26) This shell was previously reported in sediments from other NRZs on the Rifle floodplain,(7) indicating a high degree of similarity in U(IV) speciation between these spatially separated locations. Both the first and the second peak in the FT-EXAFS spectra were well aligned with those of the products of microbial U(VI) reduction in the

presence of *Shewanella*, where molecular complexes of U(IV) were found to be bound to biomass, most likely through P- and/or C-containing ligands (26; Figure 3b). Moreover, good LC-LS fits performed over the data range 3–8 $Å^{-1}$ with minimized Rf were obtained for U L-edge EXAFS spectra of samples from Rifle fine-grained NRZ sediments (cores 748 and 753) when fit with U(IV) complexes bound to OM-clay aggregates(29) and molecular complexes of U(IV) bound to biomass through P- and/or C-containing ligands(26) (Figure 3). Conversely, this frequency at 2.65 Å (R+dR; Figure 3b) is not present in the Bone data, suggesting that additional ligands are present in the field systems. In general, clay minerals and pyrite are more abundant in the field sediments than the model system. Consequently, it is plausible that that 2.65 Å FT peak is a Al, Si or Fe neighbor.(29, 59) In spite that further work is needed to refine the U speciation, our observations support the idea that U(IV) exists in a variety of coordination environments in the field systems. We conclude that noncrystalline U(IV) forms in the NRZs are not strongly bound and could be sensitive to remobilization.

Groundwater U Concentrations over Time

Depth-resolved groundwater samples were collected from wells NAT-M8 and NAT-M4 at the Naturita site between March and November 2015. NAT-M8 is proximal to the location of the NAT-M8–1 core, which contained a U-enriched NRZ (Figure 1c; cf. Vertical Distribution of U and Redox Conditions section). In contrast, the NAT-M4 well is located nearby NAT-M-2 and -3 cores, where NRZs and U pools were not detected (Figure SI-3). Dissolved U concentrations in the groundwater of NAT-M8 remained around 350 µg/L throughout the measurement period, except for a spike in July–August with concentrations up to 1850 µg/L. The depth interval of this spike corresponds to an observed NRZ. Simultaneous with this spike, the ORP measurements indicated highly reducing conditions (−22 mV; Figure 4a). In the groundwater at NAT-M4 (not proximal to NRZs), reducing conditions were also detected in August, which coincided with a spike in U concentration. However, U concentrations did not exceed 300 µg/L (Figure 4b,c).

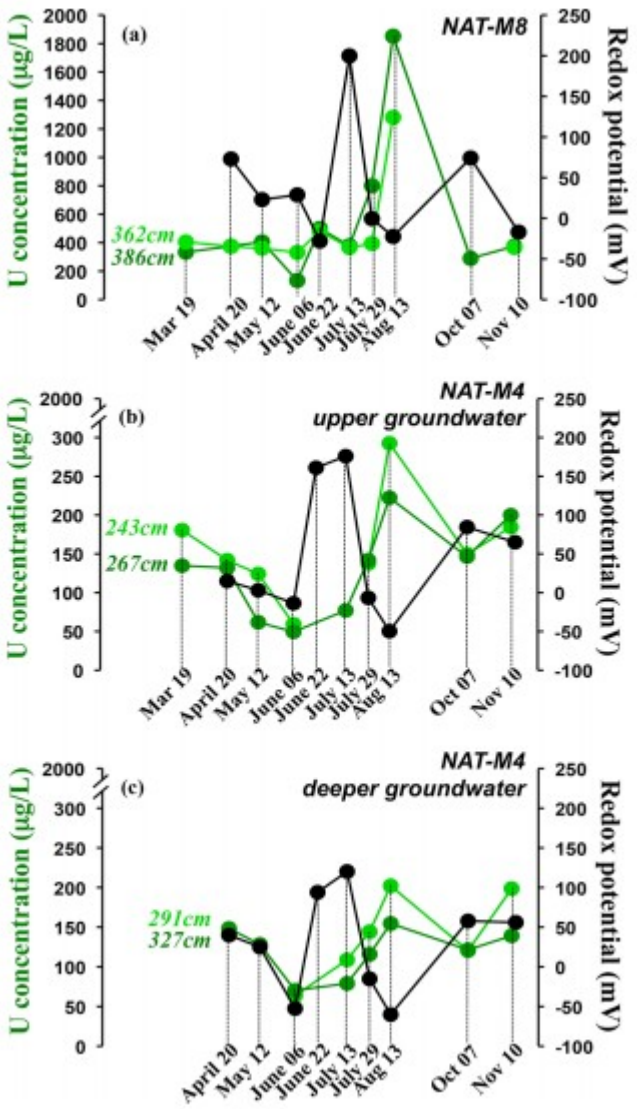

Figure 4. Evolution over time of dissolved U (green line) concentrations in groundwater at the Naturita site compared to the redox potential (black line) in well NAT-M8, which is proximal to U-enriched NRZs (a) and in the upper (b) and deeper (c) groundwater of well NAT-M4, which is located in a zone without nearby NRZ sediment. Redox potentials were measured at 380 cm in well NAT-M8, and at 250 and 325 cm depth in well NAT-M4 for upper and deeper groundwater, respectively.

This observation raises the question; can NRZs release soluble U(IV) to the aquifer? To help address this question, we analyzed U concentrations in porewater from the Rifle 753 core collected in August, which exhibited strongly reducing conditions.(9) Dissolved U concentrations increased from 4 to 12 µg/g in the aquifer sediments up to 269 µg/L in the NRZ (Table SI-1). This finding supports the idea that mobile U(IV) is present in NRZs and could be released to the aqueous phase as proposed by Wang et al.(39)

Discussion

Our examinations of sediment cores from three field sites reveals a consistent co-occurrence of U with OM and Fe-sulfides in NRZ sediments.

Recently, Bone et al.(29) and Mikutta et al.(60) have shown that surface functional groups on natural organic matter (NOM) strongly complex U(IV) and competitively inhibit the formation of UO_2. Moreover, both of these studies show that organic functional groups can outcompete mineral surface sites when both are present. In the present study, relatively high concentrations of OM were observed in the NRZs from Rifle, Naturita, and Grand Junction, which are generally consistent with the conditions examined by Bone et al.(29)NOM occurred predominantly as lignin, lipid and proteins, (61) suggesting that the majority of the organics were of microbial origin for all NRZs.(62) Moreover, the preservation of proteins within the NRZs has previously been attributed to their specific ability to interact with mineral surfaces.(61) We conclude that organic functional groups, and likely also mineral surface sites, are present at sufficiently high abundance in the Rifle, Naturita, and Grand Junction NRZs to be able to complex the majority of U(IV) that is produced under reducing conditions.

Variable Abundance of Uraninite

It has been discussed in the literature that noncrystalline U(IV) may transform directly to uraninite in natural systems. However, in the case of surface-complexed U(IV), such a mechanism is not thermodynamically supported, as it involves converting the most stable form of U(IV) under local chemical conditions (i.e., surface-complexed “noncrystalline” U(IV)) into a minority species. Nevertheless, as noted by Bone et al.,(29) thermodynamic mass action should produce small quantities of crystalline U(IV), even when surface-complexed noncrystalline U(IV) is the dominant product of U(VI) reduction. Consequently, the increasing relative abundance of crystalline U(IV) in Rifle < Naturita < Grand Junction must reflect one or both of the following: a diminishing abundance of organic surface sites relative to U(IV) and/or the presence of processes that favor phases having relatively slower oxidation/dissolution kinetics (both Naturita and Grand Junction represent coarse-grained NRZs).

Impact of Sediment Grain Size on U(IV) Speciation and Reactivity

As previously concluded in Noël et al.,(9) the exchange of solutes and flow of oxidants is relatively slow into diffusion-limited fine-grained NRZs (Figure 2). In contrast, exposure of coarse-grained NRZs to dissolved oxygen causes sulfides to be oxidized, with a disproportionate loss of mackinawite (FeS) as compared to the more stable pyrite. We propose that the sharp contrast in oxidation kinetics of noncrystalline U(IV) (relatively fast oxidation kinetics) compared to uraninite (relatively slow;(33, 34)) causes a chemical behavior analogous to that of mackinawite and pyrite. The results shown in Figures 1 and 2 show that both mackinawite and noncrystalline U(IV) are abundant in fine-grained predominantly saturated sediments due to the stability and persistence of reducing conditions. In contrast, mackinawite was largely absent(9) in the Naturita and Grand Junction coarse-grained NRZs. Concomitantly, crystalline U(IV) defined as the unextractable fraction

comprised 5–10% and 15–25% of total U, respectively (Figure 2c,d). Moreover, uraninite has previously been reported to be the dominant form of U(IV) in coarse-textured NRZ sediments.(8) Thus, enrichment of crystalline U(IV) occurs under the same (episodic) conditions that favor oxidation of mackinawite. This comparison suggests that episodic redox cycling in coarse-grained NRZs that depletes mackinawite also depletes noncrystalline U(IV), resulting in relative enrichment of crystalline U(IV) over time. This model is schematically illustrated in Figure 5c. Frequent oxidative losses would be expected to retard or limit the accumulation of U(IV), whereas the persistence of reducing conditions in fine-grained NRZs should support U(IV) accumulation (Figures 1 and SI-8) as long as inward diffusion of U(VI) is sustained.(4) Thus, our findings suggest that the relative abundances and absolute concentrations of U(IV) species could directly related to sediment properties, particularly grain size. We posit that the susceptibility of NRZ U stocks to oxidative remobilization can be predicted based on the relative abundance of mackinawite.

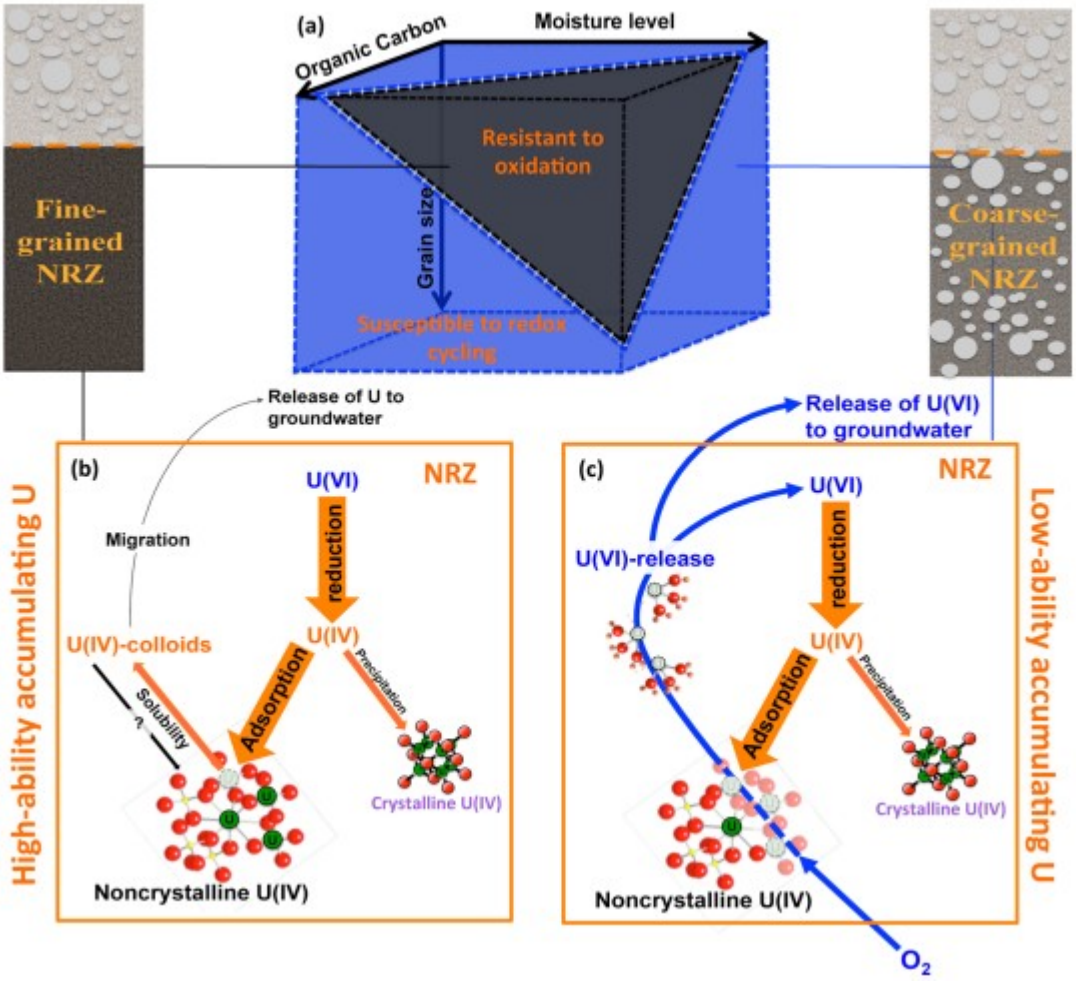

Figure 5. Illustration of the biogeochemical reaction network believed to control accumulation and longevity of U(IV) species formed in NRZs. Sediment OC content, particle size, and pore saturation, control the ability of NRZs to protect U(IV) species from oxidation (a). Oxidation-resilient NRZs develop

higher U-accumulation ability (b), whereas oxidation-susceptible NRZs exhibit lower U-accumulation ability (c). In this model, the primary oxidant is assumed to be O_2(blue line), which diffuses into oxidation-susceptible NRZs and oxidizes noncrystalline U(IV), producing U(VI) that can be rereduced or released to groundwater. This process is expected to decrease the ability of these NRZs to accumulate U(IV), and increase the crystalline U(IV) proportion relative to noncrystalline U(IV) proportion (Impact of Sediment Grain Size on U(IV) Speciation and Reactivity section). Conversely, in the absence of oxidative perturbations, U(IV) pools accumulate in persistently reduced NRZs, but may be released as U(IV)-colloids to groundwater (U(IV) Accumulation Model section).

U(IV) Accumulation Model

We propose that two conditions are necessary to accumulate and fractionate U(IV) in NRZs: (i) organic and mineral surface functional groups should be abundant relative to U,(29) and (ii) protection from oxidation. The fine-grained texture in the sulfidic organic- and clay-enriched sediments was found, in this study, to moderate the response of the system to oxidant diffusion, protecting noncrystalline U(IV) from oxidation. Oxygen consumption through microbial respiration further contributes to protecting the sediments from oxidation.(63, 64) Thus, the elevated OC content in the fine-grained NRZs contributes indirectly to protecting reduced phases such as mackinawite and noncrystalline U(IV) from oxidation. We conclude that NRZ susceptibility to oxidation is dependent on OC content and particle size (Figure 5a), allowing us to distinguish between ‘oxidation-resilient’ (Figure 5b) and ‘oxidation-susceptible’ NRZs (Figure 5c).

Oxidation of sulfides and U(IV) species corresponds with seasonal hydrological variability. Water table fluctuations that cause NRZs to become unsaturated can oxidize their internal portions.(65, 66) A lack of mackinawite or noncrystalline U(IV) suggests regular discharge of oxidized U, which could help explain seasonal increases in groundwater concentrations of U.(3, 67) U(VI) that is not discharged from NRZs could be rereduced when the anoxia is restored, possibly leading to further evolution of U pool speciation over time under fluctuating redox conditions. Moreover, it is likely that seasonal exposure of NRZs to oxidants also impacts the chemical and physical form and reactivity of the NOM,(61) which in turn could influence its affinity to bind U(IV), and thus impact the noncrystalline U(IV) molecular structure. Conversely, preservation of mackinawite and noncrystalline U(IV) is promoted by year-round saturated conditions.

Environmental Implications

Groundwater U concentrations (well NAT-M8 Naturita) show that U is released from sediments under highly reducing conditions (Figure 4), suggesting mobilization of U(IV) species in spite of the generally assumed low solubility of U(IV). Laboratory experiments with groundwater under reducing conditions suggest that U(IV) complexation with colloids may enhance its mobility.(36-38)Additional laboratory studies provide support for the formation of U(IV)-silicate colloids(57) and of U(IV)-dioxide colloids.(68) Recently, Wang et al.(39) showed that U(IV) can occur as a distinct species associated with Fe(II) and organic matter colloids in porewater from a natural wetland. These observations offer an explanation to our results,

that is, that noncrystalline U(IV) formed in an NRZ could migrate to groundwater in colloidal form (Table SI-1, Figure 5b), although the low concentrations in our porewaters prevented us from confirming the soluble U speciation by EXAFS. Thus, we conclude that oxidation-resilient NRZs may contribute to slow U loss due to reductive remobilization of U(IV), and that this possibility warrants further research.

Our current findings support the previously proposed(4) hypothesis that sulfidic organic-enriched sediments play a regional role in U(IV) storage and U plume longevity in UCRB floodplains. Ref 58.

Acknowledgment

Research was supported by the DOE-BER Climate and Environmental Sciences Division through the SLAC Science Focus Area (SFA) program and by DOE-BES through its support for SSRL. SSRL and SLAC are supported by the U.S. Department of Energy, Office of Science, Office of Basic Energy Sciences under Contract No. DE-AC02-76SF00515, the DOE Office of Biological and Environmental Research, and by the National Institutes of Health, National Institute of General Medical Sciences (including P41GM103393). Coring and field site access was provided by U.S. Department of Energy (DOE)-Legacy Management. Field work at the Rifle site was partially supported by the Lawrence Berkeley National Laboratory's Genomes-to-Watershed Scientific Focus Area. U.S. DOE, Office of Science, Office of Biological and Environmental Research funded the work under contract DE-AC02-05CH11231 (Lawrence Berkeley National Laboratory; operated by the University of California). The Canadian Light Source (CLS) is supported by the Natural Sciences and Engineering Research Council of Canada, the National Research Council Canada, the Canadian Institutes of Health Research, the Province of Saskatchewan, Western Economic Diversification Canada, and the University of Saskatchewan. We thank Craig Goodknight, Dick Dayvault, David Traub, Sam Campbell, David Miller, Sandy Beranich, David Atkinson, Dan Sellers, David Dander, Rob Rice, Anthony Martinez, Jennifer Graham, Jeff Price, and Gretchen Baer of Navarro Research and Engineering, Inc., for their assistance with planning and conducting field sampling activities. We especially thank William Dam (U.S. DOE-Legacy Management), Ray Johnson, and Sarah Morris (Navarro Research and Engineering, Inc.) for their help to manage the field sampling activities and to storage and shipping of samples. We thank the SLAC radiation protection program for their assistance with radioactive sample handling. Ryan Davis and the technical staff at SSRL are also acknowledged for their technical support during XAS measurements. The authors thank also Cynthia Patty (SLAC) for her great help in the preparation of field sampling activities and laboratory activities, Guangchao Li (Stanford University) for his help during analyses by ICP, and Lilia Barragan for her help for the preparation of samples to analyze by XRF and elemental analyzer. And finally, we especially thank Jeff Maske (SLAC) to help to manufacture the peeper structure.

References

(1) Riley, R. G.; Zachara, J. M.; Wober, F. J. Chemical Contaminants on DOE Lands and Selection of Contaminant Mixtures for Subsurface Science Research; DOE Office of Energy Research: Washington, DC, 1999; p 77. (2) Hazen, T.; Faybishenko, B.; Jordan, P. Complexity of Groundwater Contaminants at DOE Sites; Lawrence Berkeley National Laboratory, 2011; p 58. (3) Zachara, J. M.; Long, P. E.; Bargar, J. R.; Davis, J. A.; Fox, P. M.; Fredrickson, J. K.; Freshley, M. D.; Konopka, A. E.; Liu, C.; McKinley, J. P.; Rockhold, M. L.; Williams, K. H.; Yabusaki, S. B. Persistence of uranium groundwater plumes: contrasting mechanisms at two DOE sites in the groundwater-river interaction zone. J. Contam. Hydrol. 2013, 147, 45−72. (4) Janot, N.; Lezama-Pacheco, J. S.; Pham, D. Q.; O'Brien, T. M.; Hausladen, D.; Noel, V.; Lallier, F.; Maher, K.; Fendorf, S.; Williams,¨ K. H.; Long, P. E.; Bargar, J. R. Physico-chemical heterogeneity of organic-rich sediments in the Rifle aquifer, CO: Impact on uranium biogeochemistry. Environ. Sci. Technol. 2016, 50 (1), 46−53. (5) Dam, W. L.; Campbell, S.; Johnson, R. H.; Looney, B. B.; Denham, M. E.; Eddy-Dilek, C. A.; Babits, S. J. Refining the site conceptual model at a former uranium mill site in Riverton, Wyoming, USA. Environ. Earth Sci. 2015, 74 (10), 7255−7265. (6) Johnson, R. H.; Dam, W. L.; Campbell, S.; Noel, V.; Bone, S. E.;¨ Bargar, J. R.; Dayvault, J. Persistent secondary contaminant sources at a former uranium mill site, Riverton, Wyoming USA, Mining Meets Water − Conflicts and Solutions. Proceedings IMWA, Freiberg/ Germany, 2016. (7) Campbell, K. M.; Kukkadapu, R. K.; Qafoku, N. P.; Peacock, A. D.; Lesher, E.; Williams, K. H.; Bargar, J. R.; Wilkins, M. J.; Figueroa, L.; Ranville, J. F.; Davis, J. A.; Long, P. E. Geochemical, mineralogical and microbiological characteristics of sediment from a naturally reduced zone in a uranium-contaminated aquifer. Appl. Geochem. 2012, 27 (8), 1499−1511. (8) Qafoku, N. P.; Gartman, B. N.; Kukkadapu, R. K.; Arey, B. W.; Williams, K. H.; Mouser, P. J.; Heald, S. M.; Bargar, J. R.; Janot, N.; Yabusaki, S.; Long, P. E. Geochemical and mineralogical investigation of uranium in multi-element contaminated, organic-rich subsurface sediment. Appl. Geochem. 2014, 42, 77−85. (9) Noel, V.; Boye, K.; Kukkadapu, R. K.; Bone, S.; Lezama-Pacheco,¨ J. S.; Cardarelli, E.; Janot, N.; Fendorf, S.; Williams, K. H.; Bargar, J. R. Understanding controls on redox processes in floodplain sediments of the Upper Colorado River Basin. Sci. Total Environ. 2017, 603-604, 663−675. (10) Liger, E.; Charlet, L.; Van Cappellen, P. Surface catalysis of uranium(VI) reduction by iron(II). Geochim. Cosmochim. Acta 1999, 63, 2939−2955. (11) Behrends, T.; Van Cappellen, P. Competition between enzymatic and abiotic reduction of uranium(VI) under iron reducing conditions. Chem. Geol. 2005, 220, 315−327. (12) Jeon, B.-H.; Dempsey, B. A.; Burgos, W. D.; Barnett, M. O.; Roden, E. E. Chemical reduction of U(VI) by Fe(II) at the solid-water interface using natural and synthetic Fe(III) oxides. Environ. Sci. Technol. 2005, 39, 5642−5649. (13) Ilton, E. S.; Heald, S. M.; Smith, S. C.; Elbert, D.; Liu, C. Reduction of uranyl in the interlayer region of low iron micas under anoxic and aerobic conditions. Environ. Sci. Technol.

2006, 40, 5003− 5009. (14) Hua, B.; Deng, B. Reductive immobilization of uranium(VI) by amorphous iron sulfide. Environ. Sci. Technol. 2008, 42 (23), 8703− 8708. (15) Jang, J.-H.; Dempsey, B. A.; Burgos, W. D. Reduction of U(VI) by Fe(II) in the presence of hydrous ferric oxide and hematite: effects of solid transformation, surface coverage, and humic acid. Water Res. 2008, 42, 2269−2277. (16) Nico, P. S.; Stewart, B. D.; Fendorf, S. Incorporation of oxidized uranium into Fe (hydr)oxides during Fe(II) catalyzed remineralization. Environ. Sci. Technol. 2009, 43, 7391−7396. (17) Chakraborty, S.; Favre, F.; Banerjee, D.; Scheinost, A. C.; Mullet, M.; Ehrhardt, J.-J.; Brendle, J.; Vidal, L.; Charlet, L. U(VI) sorption and reduction by Fe(II) sorbed on montmorillonite. Environ. Sci. Technol. 2010, 44, 3779−3785. (18) Boland, D. D.; Collins, R. N.; Payne, T. E.; Waite, T. D. Effect of amorphous Fe(III) oxide transformation on the Fe(II)-mediated reduction of U(VI). Environ. Sci. Technol. 2011, 45, 1327−1333. (19) Hyun, S. P.; Davis, J. A.; Sun, K.; Hayes, K. F. Uranium(VI) reduction by iron(II) monosulfide mackinawite. Environ. Sci. Technol. 2012, 46 (6), 3369−3376. (20) Veeramani, H.; Scheinost, A. C.; Monsegue, N.; Qafoku, N. P.; Kukkadapu, R.; Newville, M.; Lanzirotti, A.; Pruden, A.; Murayama, M.; Hochella, M. F. Abiotic reductive immobilization of U(VI) by biogenic mackinawite. Environ. Sci. Technol. 2013, 47, 2361−2369. (21) Lovley, D. R.; Phillips, E. J. P.; Gorby, Y. A.; Landa, E. R. Microbial reduction of uranium. Nature 1991, 350 (6317), 413−416. (22) Lovley, D. R.; Phillips, E. J. P. Reduction of uranium by Desulfovibrio desulfuricans. Appl. Environ. Microbiol. 1992, 58 (3), 850− 856. (23) Cai, C. F.; Dong, H.; Lia, H.; Xiao, X.; Ou, G.; Zhang, C. Mineralogical and geochemical evidence for coupled bacterial uranium mineralization and hydrocarbon oxidation in the Shashagetai deposit, NW China. Chem. Geol. 2007a, 236 (1−2), 167−179. (24) Cai, C. F.; Li, H.; Qin, M.; Luoa, X.; Wang, F.; Ou, G. Biogenic and petroleum-related ore-forming processes in Dong-sheng uranium deposit, NW China. Ore Geol. Rev. 2007b, 32 (1−2), 262−274. (25) Ahmed, B.; Cao, B.; McLean, J. S.; Ica, T.; Dohnalkova, A.; Istanbullu, O.; Paksoy, A.; Fredrickson, J. K.; Beyenal, H. Fe(III) reduction and U(VI) immobilization by Paenibacillus sp. Strain 300A, isolated from Hanford 300A subsurface sediments. Appl. Environ. Microbiol. 2012, 78 (22), 8001−9. (26) Bernier-Latmani, R.; Veeramani, H.; Junier, P.; Lezama-Pacheco, J.; Suvorova, E. I.; Sharp, J. O.; Wigginton, N. S.; Bargar, J. R. Nonuraninite products of microbial U(VI) reduction. Environ. Sci. Technol. 2010, 44 (24), 9456−9462. (27) Fletcher, K. E.; Boyanov, M. I.; Thomas, S. H.; Wu, Q.; Kemmer, K. M.; Löffler, F. E. U(VI) reduction to mononuclear U(IV) by Desulfitobacterium species. Environ. Sci. Technol. 2010, 44 (12), 4705−4709. (28) Ray, A. E.; Bargar, J. R.; Sivaswamy, V.; Dohnalkova, A. C.; Fujita, Y.; Peyton, B. M.; Magnuson, T. S. Evidence for multiple modes of uranium immobilization by an anaerobic bacterium. Geochim. Cosmochim. Acta 2011, 75 (10), 2684−2695. (29) Bone, S. E.; Dynes, J. J.; Cliff, J.; Bargar, J. R. Uranium(IV) adsorption by natural organic matter in anoxic sediments. Proc. Natl. Acad. Sci. U. S. A. 2017, 114 (4), 711−716. (30) Bargar, J. R.; Williams, K. H.; Campbell, K. M.; Long, P. E.; Stubbs, J. E.; Suvorova, E. I.;

Lezama-Pacheco, J. S.; Alessi, D. S.; Stylo, M.; Webb, S. M.; Davis, J. A.; Giammar, D. E.; Blue, L. Y.; BernierLatmani, R. Uranium redox transition pathways in acetate-amended sediments. Proc. Natl. Acad. Sci. U. S. A. 2013, 110 (12), 4506−4511. (31) Gardner, P.; Solomon, D. K. Investigation of the Hydrologic Connection between the Moab Mill Tailings and the Matheson Wetland Preserve; University of Utah, Dept. of Geology and Geophysics: Salt Lake City, UT, 2003. (32) Davis, J. A.; Curtis, G. P.; Wilkins, M. J.; Kohler, M.; Fox, P. M.; Naftz, D. L.; Lloyd, J. R. Processes affecting transport of uranium in a suboxic aquifer. Phys. Chem. Earth, Parts A/B/C 2006, 31 (10−14), 548−555. (33) Cerrato, J. M.; Ashner, M. N.; Alessi, D. S.; Lezama-Pacheco, J. S.; Bernier-Latmani, R.; Bargar, J. R.; Giammar, D. E. Relative Reactivity of biogenic and chemogenic uraninite and biogenic noncrystalline U(IV). Environ. Sci. Technol. 2013, 47 (17), 9756−9763. (34) Alessi, D. S.; Lezama-Pacheco, J. S.; Stubbs, J. E.; Janousch, M.; Bargar, J. R.; Persson, P.; Bernier-Latmani, R. The product of microbial uranium reduction includes multiple species with U(IV)−phosphate coordination. Geochim. Cosmochim. Acta 2014, 131, 115−127. (35) Wang, X.; Johnson, T. M.; Lundstrom, C. C. Isotope fractionation during oxidation of tetravalent uranium by dissolved oxygen. Geochim. Cosmochim. Acta 2015, 150, 160−170. (36) Ollila, K.; Olin, M.; Lipponen, M. Solubility and oxidation state of uranium under anoxic conditions (N2 atmosphere). Radiochim. Acta 1996, 74 (s1), 9−13. (37) Noseck, U.; Brasser, T.; Laciok, A.; Hercik, M.; Woller, F. Uranium Migration in Argillaceous Sediments As Analogue for Transport Processes in the Far Field of Repositories (Ruprechtov site, Czech Republic). In Uranium in the Aquatic Environment: Proceedings of the International Conference Uranium Mining and Hydrogeology III and the International Mine Water Association Symposium Freiberg, Germany; Merkel, B. J., Planer-Friedrich, B., Wolkersdorfer, C., Eds.; Springer-Verlag: Berlin, Germany, 2002; pp 207−215. (38) Delecaut, G.; Maes, N.; De Canniere, P.; Wang, L. Effect of reducing agents on the uranium concentration above uranium(IV) amorphous precipitate in Boom Clay pore water. Radiochim. Acta 2004, 92 (9), 545−550. (39) Wang, Y.; Frutschi, M.; Suvorova, E.; Phrommavanh, V.; Descotes, M.; Osman, A. A.; Geipel, G.; Bernier-Latmani, R. Mobile uranium(IV)-bearing colloids in a mining-impacted wetland. Nat. Commun. 2013, DOI: 10.1038/ncomms3942. (40) DOE Grand Junction Office. Final Site Observational Work Plan for the UMTRA Project Old Rifle Site. 1999. (41) DOE. Environmental assessment of ground water compliance at the Naturita, Colorado, UMTRA project site. Work performed under DOE contract No. DE-AC13-02GJ79491. 2003. (42) DOE-LM Long-term surveillance and maintenance plan for the Grand Junction, Colorado, site. DOE-LM/GJ1164 − 2006. (S.M. Stoller Corp., Grand Junction, CO). 2006. (43) DOE Legacy management. Rifle, CO. Processing sites and disposal site - Fact Sheet. 2011. (44) DOE Legacy management. Fact Sheet. Rifle, Colorado, processing sites and disposal site. DOE-LM, Grand Junction, CO). 2013. (45) Anderson, R. T.; Vrionis, H. A.; Ortiz-bernad, I.; Resch, C. T.; Long, P. E.; Dayvault, R. D.; Karp, K.; Marutzky, S.; Metzler, D. R.; Peacock, A. D.; White, D. C.; Lowe, M.; Lovley,

D. R. Stimulating the in situ activity of Geobacter species to remove uranium from the groundwater of a uranium-contaminated aquifer. Appl. Environ. Microbiol. 2003, 69 (10), 5884−5891. (46) Robinson, P. Uranium mill tailings remediation performed by the US DOE: an overview. report for Uranium Impact Assessment Program. 2004 (http://www.sric.org/). (47) Yabusaki, S. B.; Fang, Y.; Williams, K. H.; Murray, C. J.; Ward, A. L.; Dayvault, R. D.; Waichler, S. R.; Newcomer, D. R.; Spane, F. A.; Long, P. E. Variably saturated flow and multicomponent biogeochemical reactive transport modeling of a uranium bioremediation field experiment. J. Contam. Hydrol. 2011, 126 (3−4), 271−290. (48) Williams, K. H.; Long, P. E.; Davis, J. A.; Wilkins, M. J.; N'Guessan, A. L.; Steefel, C. I.; Yang, L.; Newcomer, D. R.; Spane, F. A.; Kerkhof, L. J.; Mcguinness, L.; Dayvault, R.; Lovley, D. R. Acetate availability and its influence on sustainable bioremediation of uraniumcontaminated groundwater. Geomicrobiol. J. 2011, 28 (5−6), 519−539. (49) Song, J.; Luo, Y. M.; Zhao, Q. G.; Christie, P. Novel use of soil moisture samplers for studies on anaerobic ammonium fluxes across lake sediment − water interfaces. Chemosphere 2003, 50, 711−715. (50) Johnston, S. G.; Burton, E. D.; Keene, A. F.; Bush, R. T.; Sullivan, L. A.; Isaacson, L. Pore water sampling in acid sulfate soils: a new peeper method. J. Environ. Qual. 2009, 38, 2474−2477. (51) Alessi, D. S.; Uster, B.; Veeramani, H.; Suvorova, E. I.; LezamaPacheco, J. S.; Stubbs, J. E.; Bargar, J. R.; Bernier-Latmani, R. Quantitative separation of monomeric U(IV) from UO2 in products of U(VI) reduction. Environ. Sci. Technol. 2012, 46, 6150−6157. (52) Ravel, B.; Newville, M. ATHENA, ARTEMIS, HEPHAESTUS: data analysis for X-ray absorption spectroscopy using IFEFFIT. J. Synchrotron Radiat. 2005, 12, 537−541. (53) Schofield, E. J.; Veeramani, H.; Sharp, J. O.; Suvorova, E.; Bernier-Latmani, R.; Mehta, A.; Stahlman, J.; Webb, S. M.; Clark, D. L.; Conradson, S. D.; Ilton, E. S.; Bargar, J. R. Structure of biogenic uraninite produced by Shewanella oneidensis strain MR-1. Environ. Sci. Technol. 2008, 42, 7898−7904. (54) Singer, D. M.; Farges, F.; Brown, G. E., Jr. Biogenic nanoparticulate UO2: Synthesis, characterization, and factors affecting surface reactivity. Geochim. Cosmochim. Acta 2009, 73, 3593−3611. (55) Tockner, K.; Stanford, J. A. Riverine flood plains: present state and future trends. Environ. Conserv. 2002, 29, 308−330. (56) Sharp, J. O.; Schofield, J.E; Veeramani, H.; Suvorova, E. I.; Kennedy, D. W.; Marshall, M. J.; Metha, A.; Bargar, J. R.; BernierLatmani, R. Structural similarities between biogenic uraninites produced by phylogenetically and m,etabolically diverse bacteria. Environ. Sci. Technol. 2009, 43 (21), 8295−8301. (57) Dreissig, I.; Weiss, S.; Hennig, C.; Bernhard, G.; Zanker, H. Formation of uranium(IV)-silica colloids at near-neutral pH. Geochim. Cosmochim. Acta 2011, 75, 352−367. (58) Bargar, J. R.; Reitmeyer, R.; Lenhart, J. J.; Davis, J. A. Characterization of U(VI)-carbonato ternary complexes on hematite: EXAFS and electrophoretic mobility measurements. Geochim. Cosmochim. Acta 2000, Volume 64 (16), 2737−2749. (59) Qafoku, N. P.; Kukkadapu, R. K.; McKinley, J. P.; Arey, B. W.; Kelly, S. D.; Wang, C.; Resch, C. T.; Long, P. E. Uranium in framboidal pyrite from a naturally bioreduced alluvial sediment. Environ. Sci. Technol. 2009, 43, 8528−8534.

(60) Mikutta, C.; Langner, P.; Bargar, J. R.; Kretzschmar, R. Tetraand Hexavalent Uranium Forms Bidentate-Mononuclear Complexes with Particulate Organic Matter in a Naturally Uranium-Enriched Peatland. Environ. Sci. Technol. 2016, 50 (19), 10465−10475. (61) Boye, K.; Noel, V.; Tfaily, M. M.; Bone, S. E.; Williams, K.;¨ Bargar, J. R.; Fendorf, S. Thermodynamically controlled preservation of organic carbon in floodplain. Nat. Geosci. 2017, 10, 415−419. (62) Ingraham, J. L.; Maaloe, O.; Neidhardt, F. C. Composition, Organization, And Structure of the Bacterial Cell. In Growth of the Bacterial Cell; Sinauer Associates Inc.: Sunderland, Mass, 1983, Chapter 1. pp 1−48. (63) Li, L.; Steefel, C. I.; Williams, K. H.; Wilkins, M. J.; Hubbard, S. S. Mineral transformation and biomass accumulation associated with uranium bioremediation at Rifle, Colorado. Environ. Sci. Technol. 2009, 43 (14), 5429−5435. (64) Bone, S. E.; Cahill, M. R.; Jones, M. M.; Fendorf, S.; Davis, J.; Williams, K. H.; Bargar, J. R. Oxidative uranium release from anoxic sediments under diffusion-limited conditions. Environ. Sci. Technol. In press.201710.1021/acs.est.7b02241 (65) Lynch, S. F. L.; Batty, L. C.; Byrne, P. Environmental risk of metal mining contaminated river bank sediment at redox-transitional zones. Minerals 2014, 4, 52−73. (66) Schulz-Zunkel, C.; Jö rg Rinklebe, J.; Bork, H.-R. Trace element release patterns from three floodplain soils under simulated oxidized− reduced cycles. Ecological Engineering. 2015, 83, 485−495. (67) Maher, K.; Bargar, J. R.; Brown, G. E., Jr. Environmental speciation of actinides. Inorg. Chem. 2013, 52 (7), 3510−3532. (68) Opel, K.; Weiss, S.; Hubener, S.; Zanker, H.; Bernhard, G. Study of the solubility of amorphous and crystalline uranium dioxide by combined spectroscopic methods. Radiochim. Acta 2007, 95 (3), 143− 149.